



Article

Exploration of Diazaspiro Cores as Piperazine Bioisosteres in the Development of σ_2 Receptor Ligands

Kuiying Xu ¹, Chia-Ju Hsieh ¹ , Ji Youn Lee ¹, Aladdin Riad ¹, Nicholas J. Izzo ² , Gary Look ², Susan Catalano ² and Robert H. Mach ^{1,*}

¹ Department of Radiology, Perelman School of Medicine, University of Pennsylvania, Philadelphia, PA 19104, USA; kuxu@penncmedicine.upenn.edu (K.X.); chiahs@penncmedicine.upenn.edu (C.-J.H.); leejyo@penncmedicine.upenn.edu (J.Y.L.); alriad@penncmedicine.upenn.edu (A.R.)

² Cognition Therapeutics Inc., Pittsburgh, PA 15203, USA; nizzo@cogrx.com (N.J.I.); glook@cogrx.com (G.L.); scatalano@cogrx.com (S.C.)

* Correspondence: rmach@penncmedicine.upenn.edu

Abstract: A series of σ_2 R compounds containing benzimidazolone and diazacycloalkane cores was synthesized and evaluated in radioligand binding assays. Replacing the piperazine moiety in a lead compound with diazaspiroalkanes and the fused octahydropyrrolo[3,4-b] pyrrole ring system resulted in a loss in affinity for the σ_2 R. On the other hand, the bridged 2,5-diazabicyclo[2.2.1]heptane, 1,4-diazepine, and a 3-aminoazetidone analog possessed nanomolar affinities for the σ_2 R. Computational chemistry studies were also conducted with the recently published crystal structure of the σ_2 R/TMEM97 and revealed that hydrogen bond interactions with ASP29 and π -stacking interactions with TYR150 were largely responsible for the high binding affinity of small molecules to this protein.

Keywords: sigma-2 receptors; TMEM97; diazaspiro cores; bioisosteres



Citation: Xu, K.; Hsieh, C.-J.; Lee, J.Y.; Riad, A.; Izzo, N.J.; Look, G.; Catalano, S.; Mach, R.H. Exploration of Diazaspiro Cores as Piperazine Bioisosteres in the Development of σ_2 Receptor Ligands. *Int. J. Mol. Sci.* **2022**, *23*, 8259. <https://doi.org/10.3390/ijms23158259>

Academic Editors: Tangui Maurice and Carmen Abate

Received: 27 June 2022

Accepted: 21 July 2022

Published: 27 July 2022

Publisher's Note: MDPI stays neutral with regard to jurisdictional claims in published maps and institutional affiliations.



Copyright: © 2022 by the authors. Licensee MDPI, Basel, Switzerland. This article is an open access article distributed under the terms and conditions of the Creative Commons Attribution (CC BY) license (<https://creativecommons.org/licenses/by/4.0/>).

1. Introduction

Sigma receptors are a class of proteins that are gaining increased importance in cell biology. Although they were initially thought to be a member of the opioid receptor family, it is now known that they belong to a discrete class of proteins. It is well established that there are two subtypes in sigma receptors, which are termed sigma-1 (σ_1 R) and sigma-2 (σ_2 R) receptors [1]. The σ_1 R has been well characterized; for example, it was first cloned in 1996 [2] and the crystal structure of this protein was reported by Kruse et al. in 2016 [3]. The σ_1 R is a 223 amino acid trans-membrane protein that is implicated in a range of biological functions, which include InsP3R-dependent calcium influx from the endoplasmic reticulum (ER) to mitochondria, lipid dynamics, mitochondrial-associated membrane stability, regulation of the ER stress response, and modulating channel and GPCR receptor function in the plasma membrane [4]. This unique range of biological functions is associated with the ability of the σ_1 R to serve as a binding partner in the formation of protein–protein interactions, with numerous “client proteins”.

The characterization of σ_2 R has been far more elusive. Initial studies relied on in vitro binding studies using [³H]DTG in the presence of (+)-pentazocine to mask σ_1 R sites and largely focused on the density of this protein in various tissues and in cancer cells grown under cell culture conditions [5,6]. The observation that this protein is expressed in high density in a wide variety of cancer cells, and that the density of the σ_2 R is higher in proliferating versus quiescent breast cancer cells, ushered in an era that focused on the development of σ_2 R ligands in the treatment and molecular imaging of cancer [7]. It was subsequently observed that antagonists of the σ_2 R were able to block the neuronal uptake of A β oligomers in cultured neurons, which led to the exploration of σ_2 R ligands as potential drugs for delaying the clinical progression of Alzheimer's disease (AD) [8]. Other

pharmacological activity associated with the σ 2R included the treatment of neuropathic pain, alcohol abuse, and cocaine abuse [9–11].

In 2011, Xu et al. [12] reported that the σ 2R represented a binding site contained within a protein complex that included the progesterone receptor binding component-1 (PGRMC1), an observation that was subsequently challenged [13–15]. In 2017, the σ 2R was purified and cloned by Kruse et al., who correctly identified this protein as the endoplasmic reticulum (ER)-resident membrane protein TMEM97 [16]. Since TMEM97 is a known protein, the name of the σ 2R was subsequently changed to σ 2R/TMEM97. The confusion regarding the association between σ 2R/TMEM97 and PGRMC1 was clarified by Riad et al., who demonstrated that these two proteins form a trimeric complex with the LDL receptor and regulate the rate of LDL uptake in cancer cells [17,18]. This group subsequently demonstrated that σ 2R/TMEM97 and PGRMC1 form a protein complex with LRP receptors, which regulate the uptake of apolipoproteins in neurons. They also demonstrated that A β oligomers are taken up into cultured neurons by forming a complex with apolipoproteins and that the rate of uptake was much higher in A β oligomers bound to ApoE3, a known risk factor in AD [19]. This observation may provide a partial explanation for the ability of σ 2R antagonists to block A β oligomer uptake in neurons and their improvement in behavioral outcomes in murine models of AD. A more recent study demonstrated that σ 2R antagonists rescue neuronal dysfunction induced by alpha synuclein aggregates isolated from postmortem samples of Parkinson's disease (PD) brain [20]. These data clearly implicate σ 2R/TMEM97 as a potential drug target in delaying the disease progression in both AD and PD.

Although a wide range of structurally diverse compounds has been shown to bind with high affinity to σ 2R/TMEM97, only a limited series of compounds display preferential binding to σ 2R versus σ 1R [7]. Examples of the different classes of compounds displaying this property are shown in Figure 1 and include the 6,7-dimethoxytetrahydroisoquinoline derivatives as **RHM-4** [21], the granatane-related bicyclo-structures represented by **SV119** [22], siramesine and its structural congeners [23,24], as well as the cyclohexylpiperazine analogs represented by **PB28** [25–27]. Structurally, they all have two fragments containing an aromatic ring separated by a spacer group containing basic nitrogen, which is a key requirement for high- σ 2R affinity. In 2019, McCurdy et al. [28] developed a series of compounds as analogues of **PB28**, containing a piperazine moiety and benzimidazolone (compound **1** in Figure 1), which resulted in a dramatic improvement in the σ 2R versus σ 1R selectivity of this class of compounds. Our group previously reported that the piperazine of pharmacologically active compounds can be replaced with a di-azaspiroalkanes and other di-azabicyclic fragments and retain higher affinity for their target protein [29–31]. Inspired by these reports, we designed a new class of σ 2R compounds containing the benzimidazolone scaffold, in which a diazacycloalkane moiety is used as the amine core required for high affinity for the σ 2R. The goal of this study was to determine if a similar strategy could be used in the development of compounds having a high affinity for σ 2R. The structures of the compounds are represented by generic structure **3** in Figure 1.

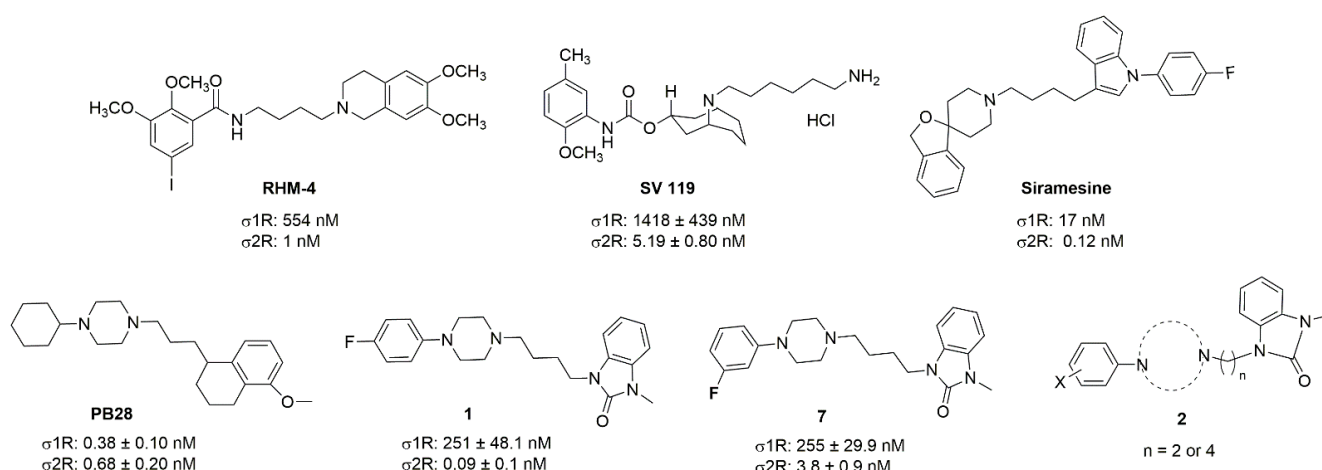
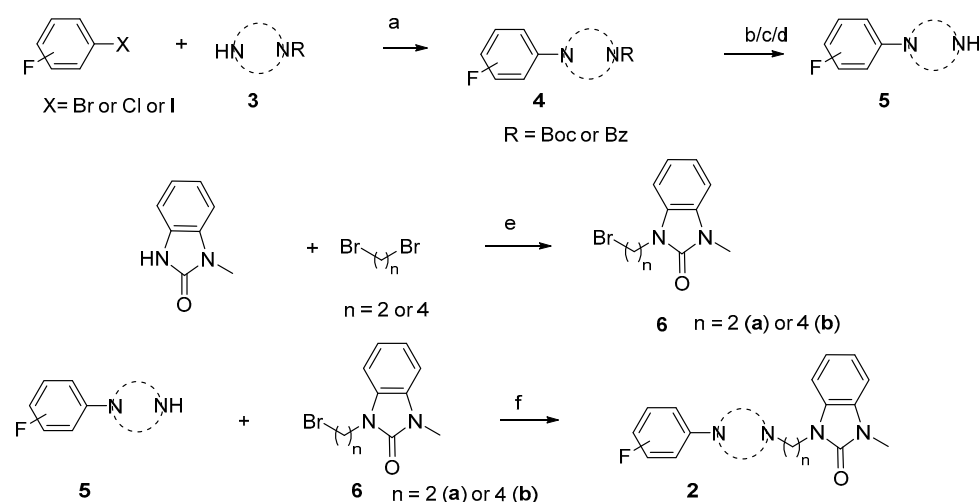


Figure 1. Structures of the σ_{2R} compounds described above.

2. Results

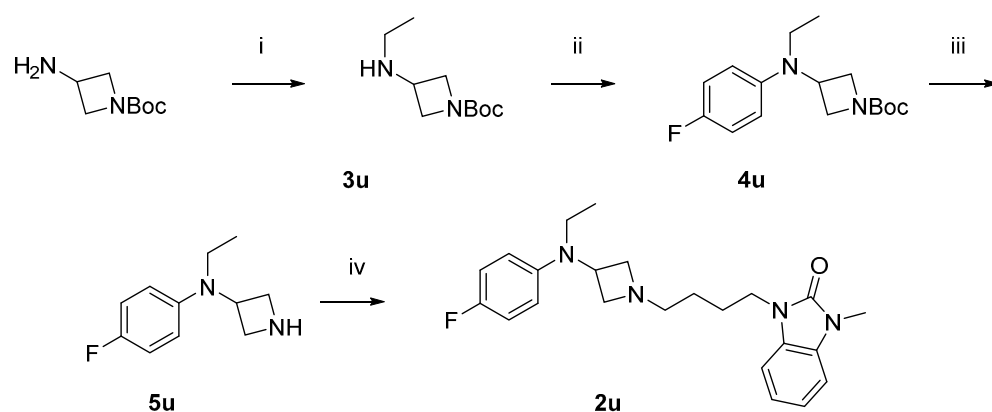
2.1. Chemistry

The synthesis of the targeting compounds began with the N-arylation of the diazaspirones or diazacycloalkanes (**3**), as outlined in Scheme 1. Protection of one of the nitrogen atoms in diazaheterocycles, with either a boc- or benzyl group followed by reaction with an aryl halide via a one-pot Pd C-N cross-coupling method [31–33], afforded high yields for the protected amines (**4**). Removal of the Boc or benzyl-protecting group provided free amines (**5**) for further coupling. This was accomplished using HCl in diethyl ether or TFA in dichloromethane. It was noted that the 2,6-diazaspiro[3.3]heptane compounds underwent a ring opening upon treatment with HCl and the TFA method was the preferred method for deprotection with this scaffold. Next, the commercially available 1-methyl-1,3-dihydro-2H-benzo[d]imidazol-2-one was alkylated with 1,2-dibromoethane or 1,4-dibromobutane to provide the bromoethyl and bromobutyl derivatives, (**6**) which were then coupled with the amines, (**5**) yielding the desired structures (**2**).



Scheme 1. General synthesis of compound **2a-u**. Reagents and conditions: (a) $\text{Pd}_2(\text{dba})_3$, RuPhos, aryl halide, NaO-t-Bu, dioxane, 100 °C, 20 min; (b) TFA, DCM, rt, 3 h; (c) 2N HCl in diethyl ether, rt, overnight; (d) $\text{H}_2/\text{Pd/C}$ in methanol; (e) NaOH, DMF, rt, overnight; and (f) K_2CO_3 , DMF, 80 °C.

Scheme 2 shows the synthesis of the compound **2u**. 1-Boc-3-aminoazetidone was ethylated with reductive amination to yield **3u**, which was then arylated with 4-fluorophenyl, giving **4u**. Removal of the Boc-protecting group afforded the free amine **5u**, which was then alkylated to yield the desired product **2u**.



Scheme 2. Synthesis of compound **2u**. Reagents and conditions: (i) CH_3CHO , $\text{NaBH}(\text{OAc})_3$, MeOH , r.t. overnight; (ii) $\text{Pd}_2(\text{dba})_3$, RuPhos , 1-bromo-4-fluorobenzene, NaO-t-Bu , dioxane, 100°C , 20 min; (iii) HCl in diethyl ether, r.t. overnight; and (iv) **6b**, K_2CO_3 , DMF , 80°C .

2.2. In Vitro Binding Assays

Radioligand binding assays were conducted using $[^{125}\text{I}]\text{RHM-4}$ with rat liver homogenates for $\sigma_2\text{R}$ -binding properties and a $\sigma_1\text{R}$ assay using $[^3\text{H}]\text{-}(+)\text{-pentazocine}$ with Guinea pig brain homogenates. Evaluation of the compounds in the in vitro radioligand binding studies was conducted using a two-step process. An initial screen for σ_1 and σ_2 receptor affinity was conducted using three different concentrations of the displacer (10 nM, 100 nM, $1\mu\text{M}$), as described previously [34]. Compounds displaying $\geq 50\%$ displacement of radioligand binding in σ_1 and σ_2 assays (Table 1) were chosen for full competition studies using 10 different concentrations of the displacer. A representative competition curve at σ_1 and σ_2 receptors is shown for compound **2t** in Figure 2. A summary of the full competition assays on hits from the three-point screening assay is provided in Table 2.

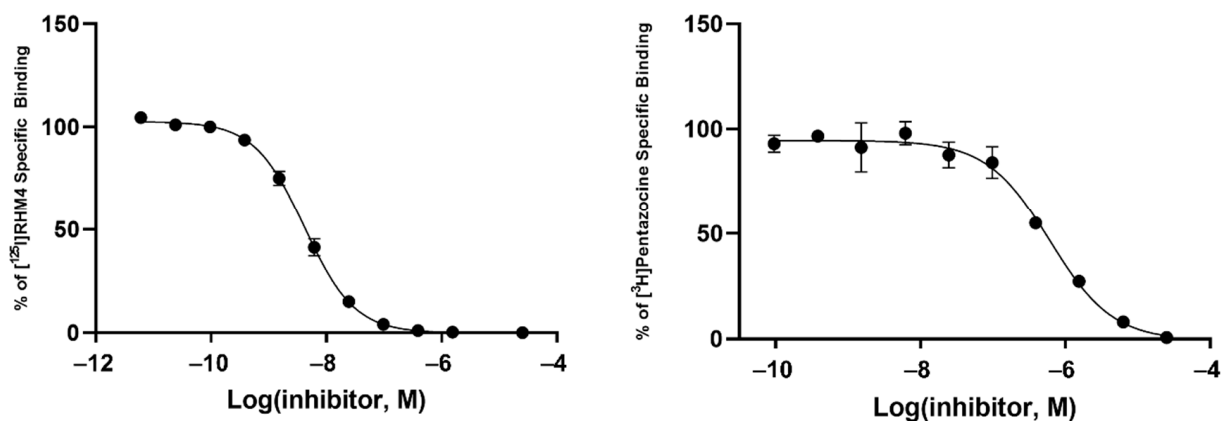


Figure 2. Representative binding curves of compound **2t** for $\sigma_2\text{R}$ (left) and $\sigma_1\text{R}$ (right).

Of the 21 analogs (**2a-u**) that were synthesized in this study, 6 were identified as “hits” in the three-point screening assay. The full competition data for the six hits revealed that replacement of the piperazine moiety with spirocyclic-diamine resulted in a reduction in affinity for $\sigma_2\text{R}$, but either no change or a modest increase in affinity for the $\sigma_1\text{R}$ (Table 1). The homopiperazine analog (**2t**) had the highest affinity for $\sigma_2\text{R}$, followed by the 2,5-diazabicyclo [2.2.1]heptane analog **2r** and the 3-(ethylamino)azetidone analog **2u**. It is also of interest to note that the other bridged analogs (i.e., **2p**, **2q**) and the fused octahydropyrrolo[3,4-b] pyrrole analog **2s** displayed a low affinity for the $\sigma_2\text{R}$.

Table 1. In vitro screening assay to identify hit compounds.

Cmpd #	X	R	n
2a	3-F		2
2b	2-F		2
2c	4-F		2
2d	3-F		4
2e	2-F		4
2f	4-F		4
2g	3-F		2
2h	2-F		2
2i	4-F		2
2j	3-F		2
2k	2-F		2
2l	4-F		2
2m	3-F		4
2n	2-F		4
2o	4-F		4
7 *	3-F		4
1 *	4-F		4
2p	4-F		4
2q	4-F		4
2r	4-F		4
2s	4-F		4
2t	4-F		4
2u	4-F		4

σ_1

σ_2

* Reference compounds

Table 2. Binding affinities of selected compounds for σ_2 and σ_1 receptors.

Cmpd #	K_i (nM) ^a		σ_1/σ_2 Ratio
	σ_2R ^b	σ_1R ^c	
2e	24.4 ± 3.3	659 ± 84.2	27
2n	41.8 ± 7.5	20.5 ± 3.3	0.5
2o	40.0 ± 3.2	45.9 ± 6.8	1.1
7 ^d	2.0 ± 0.6	702 ± 272	351
1 ^d	0.9 ± 0.1	251 ± 48.1	279
2r	10.7 ± 1.8	712 ± 135	66
2t	3.8 ± 0.9	255 ± 29.9	67
2u	18.8 ± 1.6	279 ± 30.7	15

^a Mean ± SEM, K_i values were determined by at least three experiments. ^b K_i values for σ_2R were measured on rat liver homogenates using [¹²⁵I]RHM-4 as the radioligand. ^c K_i values for σ_1R were measured on Guinea pig brain homogenates using [³H]-(+)-pentazocine as the radioligand. ^d Reference compounds [16].

2.3. Computational Chemistry Studies

The recent publication of the crystal structure of σ 2R/TMEM97 [35] allowed for the performance of a series of docking and molecular dynamic simulation studies aimed at gaining an understanding of the interactions between the compounds described above and the ligand binding site within this protein. The nitrogen atom adjacent to the carbon chain linker of the piperazine, diazepene, spirocyclic-diamine, 2,5-diazabicyclo[2.2.1]heptane, and 3-(ethylamino)azetidione is predicted to be protonated at physiological pH. The ligand-bound σ 2R/TMEM97 crystal structures suggested that the protonated high-affinity ligands form a salt bridge with ASP29 in the σ 2R-binding site [35]. Therefore, the binding pose is a salt bridge between the protonated nitrogen of the above amine moieties and ASP29 in docking studies and was considered to determine the estimated binding energy and distance between the protonated nitrogen and ASP29 (Table 3). The estimated binding energies of all the eight compounds were in a range of -10.97 to -9.65 kcal/mol and 7 was observed to have the lowest binding energy. The distances between the protonated nitrogen and ASP29 were between 2.5 and 3.3 Å.

Table 3. Docking and MDS results of selected compounds.

Cmpd #	Docking		MDS
	Distance to ASP29 (Å)	Binding Energy (kcal/mol)	Ligand RMSD (Å)
2e	3.3	-10.49	3.50 ± 0.66
2n	2.8	-10.36	3.39 ± 2.30
2o	3	-9.65	2.62 ± 0.66
7	2.5	-10.97	2.69 ± 0.33
1	2.8	-10.12	2.46 ± 0.11
2r	2.9	-10.43	3.11 ± 0.82
2t	3.2	-9.87	2.25 ± 0.32
2u	2.6	-10.5	3.24 ± 0.89

The root mean square distance (RMSD) of all compounds was calculated over 20–100 ns in five copies of the production molecular dynamics simulation (MDS) and used the first time frame (0 ns) as the reference position to evaluate the stability of the ligands in the σ 2R-binding pocket. Over the MDS production runs, compound **1**, which had the highest potency in σ 2R, showed the least movement and lowest standard deviation of RMSD (RMSD = 2.46 ± 0.11 Å) in the binding pocket (Table 3). Compound **2n**, which had the lowest binding affinity, showed a relatively large amount of motion and the highest standard deviation of RMSD (RMSD = 3.39 ± 2.30 Å) in the binding site.

An illustration of the binding pose of each compound in the σ 2R over the MDS is displayed in Figure 3. All eight selected compounds formed a salt bridge or hydrogen bond between ASP29 and the protonated nitrogen in the ligands. Compound **7**, **1**, **2r**, **2t**, and **2u** formed T-stacking between TYR150 and the protonated nitrogen in the ligands (Figure 3D–H). A cation– π interaction between TYR50 and the benzimidazolinone of the ligands was observed on **2n** and **1** (Figure 3B,E).

Summation of the overall frequency of contacts of each ligand to the binding site of σ 2R are shown in Figure 4. All eight compounds form stable interactions (frequency of contact > 0.8) with ILE24, ASP29, TYR50, GLU73, THR110, LEU111, VAL146, TYR147, and TYR150. The frequency of contact of **2n** (lowest potency for σ 2R) in the main interactive residues was observed as lower overall than other compounds and showed a high interaction with LEU46 and GLN47, two residues located at the entry of the σ 2R.

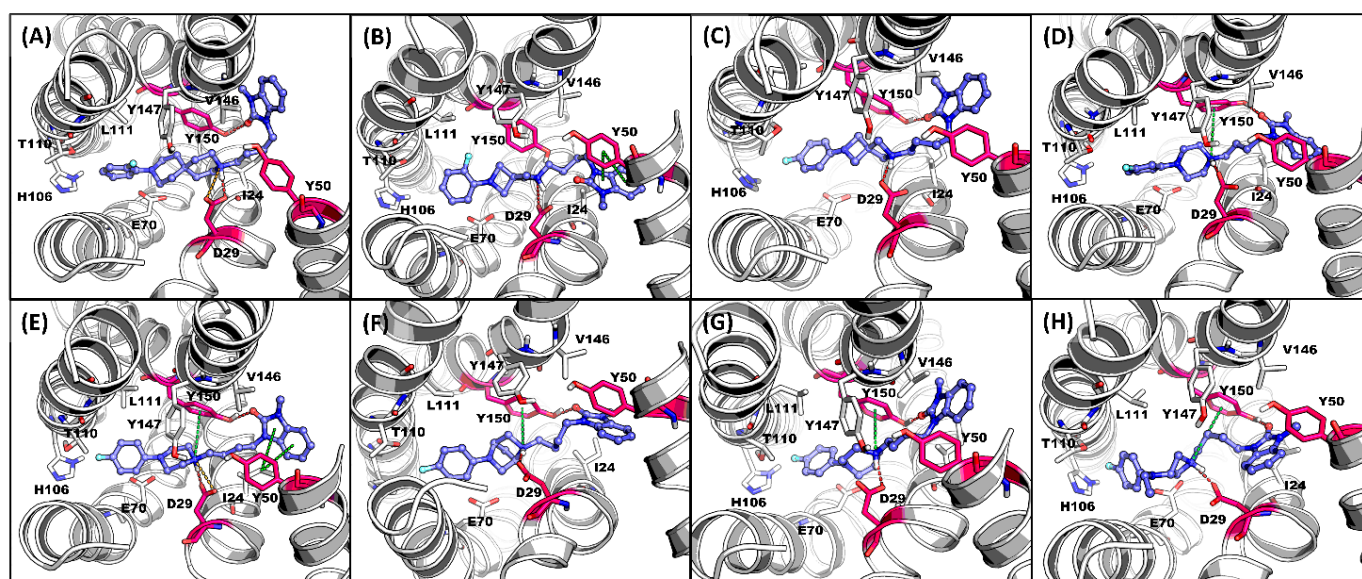


Figure 3. Representative MDS screenshot with the interactive residues in σ 2R-binding pocket for (A) **2e**, (B) **2n**, (C) **2o**, (D) **7**, (E) **1**, (F) **2r**, (G) **2t**, and (H) **2u**. H-Bond: red; salt bridge: orange; π interaction: green. Key interactive residues ASP29, TYR50, and TYR150: red.

All the selected compounds formed a hydrogen bond between ASP29 and the protonated nitrogen in the ligands and TYR150 and the oxygen at the benzimidazolinone of the ligands. Compounds having high potency for σ 2R (**1**, **2**, and **2t**; $K_i < 10$ nM) were observed forming stable hydrogen bonds with both ASP29 and TYR150 (frequency of contact > 0.90 ; Figure 5A). Compounds **2r**, **2u**, and **2e**, which had moderate binding affinities for σ 2R ($K_i = 10$ – 25 nM), showed relatively lower probability to form hydrogen bonds with ASP29 and TYR150 (frequency of contact = 0.38 – 0.97). There was no detected hydrogen bond formation between **2n** and TYR150. The average of the frequency of forming a hydrogen bond for ASP29 and TYR150 trended towards a positive correlation for σ 2R-binding affinity ($r = -0.6774$, and $p = 0.0649$; Figure 6A).

The benzimidazolinone of each ligand forms π interactions with TYR150 and TYR50 of the σ 2R. Compounds **1**, **2**, and **2t** (K_i values < 10 nM for σ 2R) formed stable π interactions with TYR150 (frequency of contact = 0.86 – 0.90), whereas compounds with lower potency for σ 2R (**2e**, **2n**, **2o**, **2r**, and **2u**; $K_i = 10$ – 42 nM) were observed as having low to moderate frequency of π interactions (0.39 – 0.75) with TYR150 (Figure 5B). Compound **2n** was the only ligand that showed a moderate probability of π interactions with TYR50 (frequency of contact = 0.60); the remaining seven compounds showed low frequency of π interactions with TYR50 (frequency of contact < 0.3). A significant correlation between the frequency of π interaction formation between TYR150 and the benzimidazolinone of the selected ligands was observed ($r = -0.8490$, and $p = 0.0077$; Figure 6B).

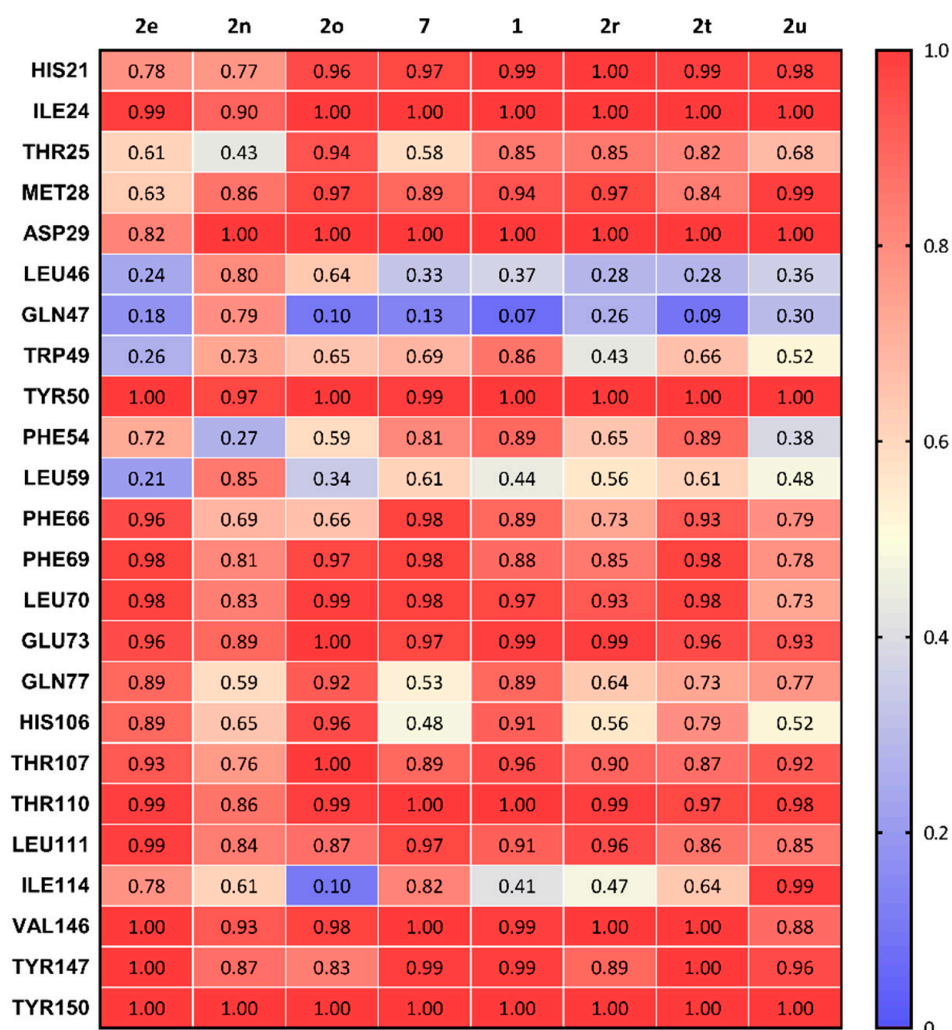


Figure 4. Summary of the frequency of all types of contacts between sigma-2 receptor and 8 compounds.

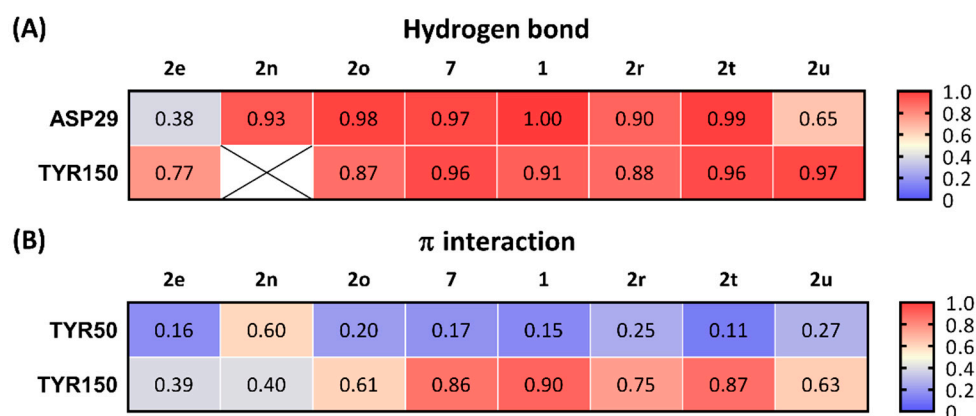


Figure 5. Frequency of contacts for three key interactions between ligands and σ 2R. (A) Hydrogen bond and (B) π interactions. : No detection of the interactions between ligand and σ 2R.

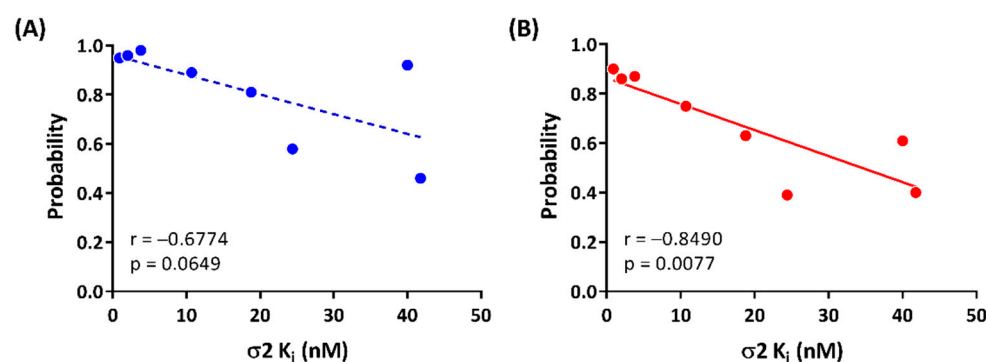


Figure 6. Correlations between σ_2R -binding affinities and (A) average of frequency of hydrogen bonds for ASP29 and TYR150 and (B) frequency of π interaction of TYR150.

3. Discussion

The goal of this study was to determine the effect of replacing the piperazine moiety of compound **1** with different isosteres, such as spirocyclic and bridged diamine ring systems. Our group previously used this strategy to synthesize compounds targeting either the dopamine D3 receptor or the DNA repair enzyme PARP-1 [29,30]. We were somewhat surprised to see that this substitution generally led to a reduction in affinity for σ_2R and an increase in affinity for σ_1R . The most potent compound in this series was the homopiperazine analog **2t**, which had an affinity of 4 nM for σ_2R and modest selectivity versus σ_1R . Another compound displaying good affinity for σ_2R and modest selectivity versus σ_1R was the bridged analog, **2r**.

Although the SAR studies did not lead to high-affinity σ_2R -selective compounds, the range of binding affinities in the compounds reported here provided a good opportunity to conduct molecular modeling studies to evaluate the properties important for interacting with this protein. Our results indicate that hydrogen bond interactions with ASP29 and π stacking interactions with TYR150 are the primary drivers of high affinity for σ_2R . These results are currently being used in docking and MDS studies to identify new scaffolds having a high affinity for σ_2R .

4. Materials and Methods

4.1. Chemistry

All reagents and solvents for synthesis were purchased and used without further purification. Structures of synthesized chemicals were identified using 1H and ^{13}C nuclear magnetic resonance (NMR) spectra and mass spectroscopy. 1H and ^{13}C NMR were recorded in units relative to deuterated solvent ($CDCl_3$) as an internal reference by Bruker DMX 500 MHz NMR instrument (Bruker, Billerica, MA, USA). 1H chemical shifts are reported in parts per million (ppm) and measured relative to tetramethylsilane (TMS). Mass spectra were acquired using a 2695 Alliance LC/MS (Milford, MA, USA). Purification of synthesized chemicals was conducted on Biotage Isolera One (Biotage, Salem, NH, USA) with a dual-wavelength UV-VIS detector. A detailed description of the synthesis and characterization of the compounds described in this paper can be found in the Supplementary Materials.

4.2. Receptor Binding Assays

For screening, [3H]-(+)-pentazocine (~50,000 cpm) or [^{125}I]RHM-4 (~200,000 cpm) was mixed with 100 nM of tested compounds. Guinea pig brain homogenates (100 μ g) or rat liver homogenates (15 μ g) were added to mixture and incubated at 37 $^\circ$ C for 90 min. The mixture was filtered by harvester and washed 3 times using cold washing buffer (10 mM Tris-HCl, 150 mM NaCl). Collected filter was mixed with 3 mL of microscintTM20 and counted 1 min/well using beta counter. To obtain specific binding affinities for sigma binding, tested compound was prepared in concentrations ranging from 10⁻⁵ to 10⁻¹¹ M using assay buffer (50 mM Tris-HCl, 0.1% bovine serum albumin (BSA), pH8) and mixed

with [^3H]-(+)-pentazocine or [^{125}I]RHM-4. After that, protein was added and incubated at 37 °C for 90 min. The bound form was filtered by Whatman CF/C filter which was soaked in 1% of polyethyleneimine (PEI) in DW and then filters were washed three times with cold washing buffer. The non-specific binding was determined in the presence of 10 μM of haloperidol or cold RHM-4. Filter was collected and read by scintillation counting (MicroBeta2[®], PerkinElmer, Beaconsfield, UK) or gamma counter (PerkinElmer, Beaconsfield, UK). The data were analyzed using PRISM 8 (GraphPad Inc., San Diego, CA, USA).

4.3. Molecular Docking

In total, 8 selected compounds including 2 references and the 6 hit compounds were used for docking and molecular dynamic studies on sigma-2 receptors. Open Babel v3.1.0 [36] was used for predicting protonated status at physiological pH of each compound. Then, the protonated structures were imported to Chem3D Ultra 15.1 (PerkinElmer Informatics, Inc., Beaconsfield, UK) and minimized using MMFF94 force field calculations for preparation for molecular docking studies. Molecular docking studies were performed via the AutoDock 4.2 [37] plugin on PyMOL (pymol.org) (accessed on 24 July 2022). The X-ray structure of σ2R /TMEM97 (PDB ID 7MFI, resolution 2.81 Å) was obtained from the RCSB Protein Data Bank (<https://www.rcsb.org/>) (accessed on 24 July 2022). Heteroatoms from water, cholesterol, and other small molecules were removed from the structure. Chain A of the four chains was extracted from the protein structure for further docking and molecular dynamics studies. Then, the protein monomer was imported to H++ web server (<http://newbiophysics.cs.vt.edu/H++>) (accessed on 24 July 2022) [38–40] to protonate the σ2R structure at pH 7.0. A grid box with dimensions of 14.6 \times 20 \times 12 Å³ was applied to the σ2R structure covering binding pocket. The Lamarckian Genetic Algorithm with a maximum of 2,500,000 energy evaluations was used to calculate 100 σ2R –ligand binding poses for each compound. The σ2R –ligand complex that reproduced the crystallographic ligand binding pose and with good docking score was reported for each compound.

4.4. Molecular Dynamics Simulation (MDS)

The positioning of proteins in membranes (PPM) web server 3.0 [41] was used to calculate the position of the membranes for σ2R . The preparation of MDS was performed on the CHARMM-GUI web server [42]. The Ligand Reader and Modeler module [43,44] was used to generate the topology and parameter files for 8 compounds. The MDS system with FF19SB force field was built by Bilayer Membrane Builder [45,46]. The protein–ligand complexes obtained from docking studies were aligned to the σ2R model generated from the PPM server and the POPC membrane was placed by the PPM σ2R model. The protein, ligand, and membrane complex was solvated in a TIP3P water box with a volume of 50 \times 50 \times 104 Å³, and then Monte-Carlo sampling was used to add 0.15M NaCl for charge neutralization.

The MDS studies were performed via Amber18 [47] on the high-performance computing (HPC) cluster at Center for Biomedical Image Computing and Analytics at the University of Pennsylvania. The input files of system minimization, 6-step equilibration, and production run for MDS were generated from the last step of Membrane Builder [45,46] on the CHARMM-GUI web server [42]. Periodic boundary conditions were used for the MDS studies. SHAKE algorithm was used to constrain bonds involving hydrogen atoms. An energy minimization of 5000 steps was implemented. Then, the minimized system was heated in a 2-step NVT ensemble with constant volume at 310 K for 125 ps with a time step of 1 fs in each step. The system was then equilibrated in a 4-step NPT ensemble at 310 K and 1 atm for total of 1625 ps (125 ps with 1 fs time step at the first step of NPT ensemble, followed by 500 ps with 2 fs time step at the second to the fourth steps of NPT ensemble). The system minimization and equilibration simulations were performed using pmemd.MPI in Amber18 [47] on 40 CPUs. Five copies of the production simulations were performed for

100 ns with a time step of 2 fs in each copy, using pmemd.cuda Amber18 [47] on NVIDIA P100 GPU.

The 20 to 100 ns of each production simulation with a total of 4000 frames (800 frames of each 5 production simulation copies) for each compound were used for further MDS analysis. The interactions between ligand and protein in the production simulations were calculated by using the software BINANA v2.1 [48].

5. Conclusions

A series of piperazine isosteres of the known σ 2R ligand **1** was synthesized and screened for activity in radioligand binding assays for sigma receptors. Although this effort did not result in the identification of high-affinity ligands for σ 2R, the wide range of affinities for this receptor provided data that could be used in computational chemistry studies aimed at determining the properties important for binding to σ 2R.

Supplementary Materials: The following supporting information can be downloaded at: <https://www.mdpi.com/article/10.3390/ijms23158259/s1>. Reference [49] are cited in the supplementary materials.

Author Contributions: Conceptualization, R.H.M., G.L. and N.J.I.; methodology, K.X., J.Y.L., C.-J.H. and A.R.; validation, R.H.M. and N.J.I.; formal analysis, K.X., J.Y.L., C.-J.H. and R.H.M.; investigation, R.H.M., S.C. and N.J.I.; resources, S.C. and N.J.I.; data curation, A.R., C.-J.H. and R.H.M.; writing—original draft preparation, K.X., C.-J.H., J.Y.L. and R.H.M.; writing—review and editing, N.J.I. and R.H.M.; supervision, R.H.M.; project administration, A.R. and R.H.M.; funding acquisition, S.C. and N.J.I. All authors have read and agreed to the published version of the manuscript.

Funding: Research reported in this publication was supported by the National Institute on Aging of the National Institutes of Health under Award Number R42AG052249. The content is solely the responsibility of the authors and does not necessarily represent the official views of the National Institutes of Health.

Institutional Review Board Statement: Not applicable.

Informed Consent Statement: Not applicable.

Data Availability Statement: The article contains complete data used to support the findings of this study.

Acknowledgments: The molecular dynamic simulation studies were conducted on a high-performance computing cluster (<https://www.med.upenn.edu/cbica/cubic.html>) (accessed on 25 July 2022) at the University of Pennsylvania Center for Biomedical Image Computing and Analytics and supported by the National Institutes of Health, Grant Number: 1S10OD023495-01.

Conflicts of Interest: Nicholas Izzo, Gary Look, and Susan Catalano are employees or have financial interest in Cognition Therapeutics, Inc. There is no conflict of interest with the other authors in this paper. The National Institutes of Health had no role in the design of the study; in the collection, analyses, or interpretation of data; in the writing of the manuscript, or in the decision to publish the results.

References

1. Bowen, W.D. Sigma receptors: Recent advances and new clinical potentials. *Pharm. Acta Helv.* **2000**, *74*, 211–218. [CrossRef]
2. Hanner, M.; Moebius, F.F.; Flandorfer, A.; Knaus, H.-G.; Striessnig, J.; Kempner, E.; Glossmann, H. Purification, molecular cloning, and expression of the mammalian sigma1-binding site. *Proc. Natl. Acad. Sci. USA* **1996**, *93*, 8072–8077. [CrossRef] [PubMed]
3. Schmidt, H.R.; Zheng, S.; Gurpinar, E.; Koehl, A.; Manglik, A.; Kruse, A.C. Crystal structure of the human sigma1 receptor. *Nature* **2016**, *532*, 527–530. [CrossRef]
4. Su, T.-P.; Hayashi, T.; Maurice, T.; Buch, S.; Ruoho, A.E. The sigma-1 receptor chaperone as an inter-organelle signaling modulator. *Trends Pharmacol. Sci.* **2010**, *31*, 557–566. [CrossRef]
5. Hellewell, S.B.; Bruce, A.; Feinstein, G.; Orringer, J.; Williams, W.; Bowen, W.D. Rat liver and kidney contain high densities of sigma-1 and sigma-2 receptors: Characterization by ligand binding and photoaffinity labeling. *Eur. J. Pharmacol.* **1994**, *268*, 9–18. [CrossRef]
6. Vilner, B.J.; John, C.S.; Bowen, W.D. Sigma-1 and sigma-2 receptors are expressed in a wide variety of human and rodent tumor cell lines. *Cancer Res.* **1995**, *55*, 408–413.

7. Mach, R.H.; Zeng, C.; Hawkins, W.G. The sigma2 receptor: A novel protein for the imaging and treatment of cancer. *J. Med. Chem.* **2013**, *56*, 7137–7160. [[CrossRef](#)]
8. Izzo, N.J.; Xu, J.; Zeng, C.; Kirk, M.J.; Mozzoni, K.; Silky, C.; Rehak, C.; Yurko, R.; Look, G.; Rishton, G.; et al. Alzheimer's therapeutics targeting amyloid beta 1-42 oligomers II: Sigma-2/PGRMC1 receptors mediate Abeta 42 oligomer binding and synaptotoxicity. *PLoS ONE* **2014**, *9*, e111899. [[CrossRef](#)]
9. Sahn, J.J.; Mejia, G.L.; Ray, P.R.; Martin, S.F.; Price, T.J. Sigma 2 receptor/Tmem97 agonists produce long lasting antineuropathic pain effects in mice. *ACS Chem. Neurosci.* **2017**, *8*, 1801–1811. [[CrossRef](#)]
10. Quadir, S.G.; Cottone, P.; Sabino, V. Role of sigma receptors in alcohol addiction. *Front. Pharmacol.* **2019**, *10*, 687. [[CrossRef](#)]
11. Aguinaga, D.; Medrano, M.; Vega-Quiroga, I.; Gysling, K.; Canela, E.I.; Navarro, G.; Franco, R. Cocaine effects on dopaminergic transmission depend on a balance between sigma-1 and sigma-2 receptor expression. *Front. Mol. Neurosci.* **2018**, *11*, 17. [[CrossRef](#)] [[PubMed](#)]
12. Xu, J.; Zeng, C.; Chu, W.; Pan, F.; Rothfuss, J.M.; Zhang, F.; Tu, Z.; Zhou, D.; Zeng, D.; Vangveravong, S.; et al. Identification of the PGRMC1 protein complex as the putative sigma-2 receptor binding site. *Nat. Commun.* **2011**, *2*, 380. [[CrossRef](#)] [[PubMed](#)]
13. Abate, C.; Niso, M.; Infantino, V.; Menga, A.; Berardi, F. Elements in support of the 'non-identity' of the PGRMC1 protein with the sigma2 receptor. *Eur. J. Pharmacol.* **2015**, *758*, 16–23. [[CrossRef](#)]
14. Chu, U.B.; Mavlyutov, T.A.; Chu, M.L.; Yang, H.; Schulman, A.; Mesangeau, C.; McCurdy, C.R.; Guo, L.W.; Ruoho, A.E. The Sigma-2 Receptor and Progesterone Receptor Membrane Component 1 are Different Binding Sites Derived From Independent Genes. *EBioMedicine* **2015**, *2*, 1806–1813. [[CrossRef](#)] [[PubMed](#)]
15. Hiranita, T. Identification of the Sigma-2 Receptor: Distinct from the Progesterone Receptor Membrane Component 1 (PGRMC1). *J. Alcohol. Drug Depend.* **2016**, *4*. [[CrossRef](#)]
16. Alon, A.; Schmidt, H.R.; Wood, M.D.; Sahn, J.J.; Martin, S.F.; Kruse, A.C. Identification of the gene that codes for the sigma2 receptor. *Proc. Natl. Acad. Sci. USA* **2017**, *114*, 7160–7165. [[CrossRef](#)]
17. Izzo, N.J.; Colom-Cadena, M.; Riad, A.A.; Xu, J.; Singh, M.; Abate, C.; Cahill, M.A.; Spires-Jones, T.L.; Bowen, W.D.; Mach, R.H.; et al. Proceedings from the fourth international symposium on σ -2 receptors: Role in health and disease. *Eneuro* **2020**, *7*. [[CrossRef](#)]
18. Riad, A.; Zeng, C.; Weng, C.C.; Winters, H.; Xu, K.; Makvandi, M.; Metz, T.; Carlin, S.; Mach, R.H. Sigma-2 Receptor/TMEM97 and PGRMC-1 Increase the Rate of Internalization of LDL by LDL Receptor through the Formation of a Ternary Complex. *Sci. Rep.* **2018**, *8*, 16845. [[CrossRef](#)]
19. Riad, A.; Lengyel-Zhand, Z.; Zeng, C.; Weng, C.C.; Lee, V.M.; Trojanowski, J.Q.; Mach, R.H. The Sigma-2 Receptor/TMEM97, PGRMC1, and LDL Receptor Complex Are Responsible for the Cellular Uptake of A β 42 and Its Protein Aggregates. *Mol. Neurobiol.* **2020**, *57*, 3803–3813. [[CrossRef](#)]
20. Limegrover, C.S.; Yurko, R.; Izzo, N.J.; LaBarbera, K.M.; Rehak, C.; Look, G.; Rishton, G.; Safferstein, H.; Catalano, S.M. Sigma-2 receptor antagonists rescue neuronal dysfunction induced by Parkinson's patient brain-derived α -synuclein. *J. Neurosci. Res.* **2021**, *99*, 1161–1176. [[CrossRef](#)]
21. Mach, R.H.; Huang, Y.; Freeman, R.A.; Wu, L.; Vangveravong, S.; Luedtke, R.R. Conformationally-flexible benzamide analogues as dopamine D₃ and sigma-2 receptor ligands. *Bioorg. Med. Chem. Lett.* **2004**, *14*, 195–202. [[CrossRef](#)] [[PubMed](#)]
22. Vangveravong, S.; Xu, J.; Zeng, C.; Mach, R.H. Synthesis of N-substituted 9-azabicyclo [3.3.1]nonan-3 α -yl carbamate analogs as sigma2 receptor ligands. *Bioorg. Med. Chem.* **2006**, *14*, 6988–6997. [[CrossRef](#)] [[PubMed](#)]
23. Moltzen, E.K.; Perregaard, J.; Meier, E. Sigma ligands with subnanomolar affinity and preference for the sigma 2 binding site. 2. Spiro-joined benzofuran, isobenzofuran, and benzopyran piperidines. *J. Med. Chem.* **1995**, *38*, 2009–2017. [[CrossRef](#)] [[PubMed](#)]
24. Perregaard, J.; Moltzen, E.K.; Meier, E.; Sanchez, C. Sigma ligands with subnanomolar affinity and preference for the sigma 2 binding site. 1. 3-(omega-aminoalkyl)-1H-indoles. *J. Med. Chem.* **1995**, *38*, 1998–2008. [[CrossRef](#)]
25. Abate, C.; Niso, M.; Lacivita, E.; Mosier, P.D.; Toscano, A.; Perrone, R. Analogues of sigma receptor ligand 1-cyclohexyl-4-[3-(5-methoxy-1,2,3,4-tetrahydronaphthalen-1-yl)propyl]piperazine (PB28) with added polar functionality and reduced lipophilicity for potential use as positron emission tomography radiotracers. *J. Med. Chem.* **2011**, *54*, 1022–1032. [[CrossRef](#)] [[PubMed](#)]
26. Berardi, F.; Abate, C.; Ferorelli, S.; Colabufo, N.A.; Perrone, R. 1-Cyclohexylpiperazine and 3,3-dimethylpiperidine derivatives as sigma-1 (s_1) and sigma-2 (s_2) receptor ligands: A review. *Cent. Nerv. Syst. Agents Med. Chem.* **2009**, *9*, 205–219. [[CrossRef](#)]
27. Abate, C.; Niso, M.; Abatematteo, F.S.; Contino, M.; Colabufo, N.A.; Berardi, F. PB28, the sigma-1 and sigma-2 receptors modulator with potent anti-SARS-CoV-2 activity: A review about its pharmacological properties and structure affinity relationships. *Front. Pharmacol.* **2020**, *11*, 589810. [[CrossRef](#)]
28. Intagliata, S.; Alsharif, W.F.; Mesangeau, C.; Fazio, N.; Seminerio, M.; Xu, Y.T.; Matsumoto, R.R.; McCurdy, C.R. Benzimidazolone-based selective sigma2 receptor ligands: Synthesis and pharmacological evaluation. *Eur. J. Med. Chem.* **2019**, *165*, 250–257. [[CrossRef](#)]
29. Reilly, S.W.; Riad, A.A.; Hsieh, C.-J.; Sahlholm, K.; Jacome, D.A.; Griffin, S.; Taylor, M.; Weng, C.-C.; Xu, K.; Kirschner, N.; et al. Leveraging a low-affinity diazaspino orthosteric fragment to reduce dopamine D₃ receptor (D₃R) ligand promiscuity across highly conserved aminergic G-protein-coupled receptors (GPCRs). *J. Med. Chem.* **2019**, *62*, 5132–5147. [[CrossRef](#)]
30. Reilly, S.W.; Puentes, L.N.; Wilson, K.; Hsieh, C.-J.; Weng, C.-C.; Makvandi, M.; Mach, R.H. Examination of Diazaspino Cores as Piperazine Bioisosteres in the Olaparib Framework Shows Reduced DNA Damage and Cytotoxicity. *J. Med. Chem.* **2018**, *61*, 5367–5379. [[CrossRef](#)]

31. Reilly, S.W.; Griffin, S.; Taylor, M.; Sahlholm, K.; Weng, C.-C.; Xu, K.; Jacome, D.A.; Luedtke, R.R.; Mach, R.H. Highly selective dopamine D3 receptor antagonists with arylated diazaspiro alkane cores. *J. Med. Chem.* **2017**, *60*, 9905–9910. [[CrossRef](#)]
32. Reilly, S.W.; Bryan, N.W.; Mach, R.H. Pd-catalyzed arylation of linear and angular spirodiamine salts under aerobic conditions. *Tetrahedron. Lett.* **2017**, *58*, 466–469. [[CrossRef](#)] [[PubMed](#)]
33. Reilly, S.W.; Mach, R.H. Pd-Catalyzed synthesis of piperazine scaffolds under aerobic and solvent-free conditions. *Org. Lett.* **2016**, *18*, 5272–5275. [[CrossRef](#)] [[PubMed](#)]
34. Kim, H.Y.; Lee, J.Y.; Hsieh, C.-J.; Riad, A.; Izzo, N.J.; Catalano, S.M.; Graham, T.J.A.; Mach, R.H. Screening of σ_2 Receptor Ligands and In Vivo Evaluation of ^{11}C -Labeled 6, 7-Dimethoxy-2-[4-(4-methoxyphenyl) butan-2-yl]-1, 2, 3, 4-tetrahydroisoquinoline for Potential Use as a σ_2 Receptor Brain PET Tracer. *J. Med. Chem.* **2022**, *65*, 6261–6272. [[CrossRef](#)] [[PubMed](#)]
35. Alon, A.; Lyu, J.; Braz, J.M.; Tummino, T.A.; Craik, V.; O'Meara, M.J.; Webb, C.M.; Radchenko, D.S.; Moroz, Y.S.; Huang, X.-P.; et al. Structures of the σ_2 receptor enable docking for bioactive ligand discovery. *Nature* **2021**, *600*, 759–764. [[CrossRef](#)]
36. O'Boyle, N.M.; Banck, M.; James, C.A.; Morley, C.; Vandermeersch, T.; Hutchison, G.R. Open Babel: An open chemical toolbox. *J. Cheminform.* **2011**, *3*, 33. [[CrossRef](#)]
37. Morris, G.M.; Huey, R.; Lindstrom, W.; Sanner, M.F.; Belew, R.K.; Goodsell, D.S.; Olson, A.J. AutoDock4 and AutoDockTools4: Automated docking with selective receptor flexibility. *J. Comput. Chem.* **2009**, *30*, 2785–2791. [[CrossRef](#)]
38. Anandakrishnan, R.; Aguilar, B.; Onufriev, A.V. H++ 3.0: Automating p K prediction and the preparation of biomolecular structures for atomistic molecular modeling and simulations. *Nucleic. Acids Res.* **2012**, *40*, W537–W541. [[CrossRef](#)]
39. Myers, J.; Grothaus, G.; Narayanan, S.; Onufriev, A. A simple clustering algorithm can be accurate enough for use in calculations of pKs in macromolecules. *Proteins* **2006**, *63*, 928–938. [[CrossRef](#)]
40. Gordon, J.C.; Myers, J.B.; Folta, T.; Shoja, V.; Heath, L.S.; Onufriev, A. H++: A server for estimating p K as and adding missing hydrogens to macromolecules. *Nucleic. Acids Res.* **2005**, *33*, W368–W371. [[CrossRef](#)]
41. Lomize, M.A.; Pogozheva, I.D.; Joo, H.; Mosberg, H.I.; Lomize, A.L. OPM database and PPM web server: Resources for positioning of proteins in membranes. *Nucleic. Acids Res.* **2012**, *40*, D370–D376. [[CrossRef](#)] [[PubMed](#)]
42. Lee, J.; Cheng, X.; Swails, J.M.; Yeom, M.S.; Eastman, P.K.; Lemkul, J.A.; Wei, S.; Buckner, J.; Jeong, J.C.; Qi, Y.; et al. CHARMM-GUI input generator for NAMD, GROMACS, AMBER, OpenMM, and CHARMM/OpenMM simulations using the CHARMM36 additive force field. *J. Chem. Theory Comput.* **2016**, *12*, 405–413. [[CrossRef](#)] [[PubMed](#)]
43. Jo, S.; Kim, T.; Iyer, V.G.; Im, W. CHARMM-GUI: A web-based graphical user interface for CHARMM. *J. Comput. Chem.* **2008**, *29*, 1859–1865. [[CrossRef](#)] [[PubMed](#)]
44. Kim, S.; Lee, J.; Jo, S.; Brooks III, C.L.; Lee, H.S.; Im, W. CHARMM-GUI ligand reader and modeler for CHARMM force field generation of small molecules. *J. Comput. Chem.* **2017**, *38*, 1879–1886. [[CrossRef](#)] [[PubMed](#)]
45. Klauda, J.B.; Venable, R.M.; Freites, J.A.; O'Connor, J.W.; Tobias, D.J.; Mondragon-Ramirez, C.; Vorobyov, I.; MacKerell Jr, A.D.; Pastor, R.W. Update of the CHARMM all-atom additive force field for lipids: Validation on six lipid types. *J. Phys. Chem. B* **2010**, *114*, 7830–7843. [[CrossRef](#)]
46. Venable, R.M.; Sodt, A.J.; Rogaski, B.; Rui, H.; Hatcher, E.; MacKerell Jr, A.D.; Pastor, R.W.; Klauda, J.B. CHARMM all-atom additive force field for sphingomyelin: Elucidation of hydrogen bonding and of positive curvature. *Biophys. J.* **2014**, *107*, 134–145. [[CrossRef](#)]
47. Case, D.; Ben-Shalom, I.; Brozell, S.; Cerutti, D.; Cheatham III, T.; Cruzeiro, V.; Darden, T.; Duke, R.; Ghoreishi, D.; Gilson, M.; et al. *AMBER 18*; University of California: San Francisco, CA, USA, 2018.
48. Durrant, J.D.; McCammon, J.A. BINANA: A novel algorithm for ligand-binding characterization. *J. Mol. Graph. Model.* **2011**, *29*, 888–893. [[CrossRef](#)]
49. Mésangeau, C.; Amata, E.; Alsharif, W.; Seminerio, M.J.; Robson, M.J.; Matsumoto, R.R.; Poupaert, J.H.; McCurdy, C.R. Synthesis and pharmacological evaluation of indole-based sigma receptor ligands. *Eur. J. Med. Chem.* **2011**, *46*, 5154–5161. [[CrossRef](#)]